Cooling System Sizing using LPTN Analysis and Multiphysics Modelling for an Axial Flux Machine and Integrated Drive

Alexander J. Jeffrey, Peter H. Connor, Gaurang Vakil, Paul Evans, Pat Wheeler, Simon Hart

***Abstract*—In this paper a Lumped Parameter Thermal Network (LPTN) is proposed for a Yokeless and Segmented Armature (YASA) axial flux permanent magnet (AFPM) machine. A simulation model is used to examine the machine in isolation, with an Integrated Motor Drive (IMD), and the machine and IMD with a remote heat sink connected using heat pipes. Losses from electrical and magnetic Finite Element Modelling (FEM) are used as inputs to the model. Introduction of the IMD is found to reduce the power rating of the machine by 27%. This performance can be returned by utilising a remote heat sink configuration to enable enlargement of the heat sink by twice the original volume.**

***Index Terms*—Axial Flux, Thermal Network, Lumped Parameter, Thermal Model, Heat Transfer, Electrical Machine, Permanent Magnet, Convection, Traction Machines**

ABREVIATIONS

IMD	Integrated Motor Drive
LPTN	Lumped Parameter Thermal Network
YASA	Yokeless and Segmented Armature
AFPM	Axial Flux Permanent Magnet
FEM	Finite Element Method
CFD	Computational Fluid Dynamics
SiC	Silicon Carbide

NOMENCLATURE

Re_θ	Rotational Reynolds Number	dimensionless
ω	Rotational Velocity	rad/s
R	Machine Radius	m
ν	Fluid Kinematic Viscosity	m^2s^{-1}
Nu	Nusselt Number	dimensionless
Pr	Prandtl Number	dimensionless
q''	Total Heat Transfer Rate	W/K
D_h	Hydraulic Diameter	m
k	Thermal Conductivity	W/mK
T	Temperature	K or ^{o}C

A. J. Jeffrey, P. H. Connor, G. Vakil, P. Evans, P. Wheeler are with the Power Electronics Machines and Control Research Group, University of Nottingham, Nottingham, United Kingdom (email:peter.connor@nottingham.ac.uk).

S. Hart is with YASA Limited, 11-14 Mead Road, Oxford Industrial Park, Yarnton, Kidlington, OX5 1QU, United Kingdom

I. INTRODUCTION

The goal of this project is to develop a high power density Integrated Motor Drive (IMD) based on an Axial Flux Permanent Magnet (AFPM) motor, utilising external air cooling as the primary cooling method. Focus will be on the Yokeless and Segmented Armature (YASA) topology [1], [2]. This paper presents a Lumped Parameter Thermal Network (LPTN) for a YASA AFPM machine. Modifications will be made to the modelling technique to include integrated power devices relevant to the type of integration being investigated. Design choices were informed using learnings from literature, including inverter module placement, heat sink design and cooling system placement. The model will include parametric cooling appropriate for single stator, double rotor YASA machines, and a coupled air-gap and rotor model to determine the heat transfer between the stator and rotor. Due to the low outer surface area of YASA machines, they are typically liquid cooled. This model will be used to predict the effectiveness of air-cooling, with heat pipes being used to relocate heat to areas where cooling volume is more readily available.

IMD's are an important development in modern electrical machines, with benefits including increased efficiency, reduced total mass and volume, and in some cases, reduced manufacturing costs [3]. As such, they are a significant step towards increasing power density for future electrical power systems. However, with the novelty of this concept comes a significant challenge in terms of system cooling. The motor and drive both produce significant thermal losses, which require a combined thermal management system to maintain suitable operating temperatures.

Thermal modelling of electrical machines and drives is an important aspect of the design process. By building computational models, it is possible to predict a large portion of the design process that would previously have been taken up by prototyping and experimental testing. This both reduces costs, and increases the speed of the design process. The most common methods of machine thermal modelling are the Finite Element Method (FEM), and LPTNs [4]. FEM utilises a Computer Aided Design model, which is meshed into a cell structure for iterative calculation of the desired physics type. FEM is typically used in combination with Computational Fluid Dynamics (CFD) to create a more comprehensive model of the machine [5]. However, these methods are computationally intensive and require highly

skilled users in order to be effective. LPTN's rely on building a representative network for the system using lumped parameter nodes. This can be processed either through a matrix calculation method, or using a network simulation software. LPTN's are an attractive alternative to FEM as they can typically be done with far lower computational effort, using more readily available software, and by users with less specialist training.

Axial Flux Permanent Magnet (AFPM) machines have recently started to be examined more closely due to their significant benefits in terms of power and torque density [2], [6]. This has in turn led to developments in Axial Flux IMD's using variations of the AFPM topology [7]. As such, some authors have begun to develop LPTN's for these machines [4], [5]. The models presented in literature utilise both mathematical and LPTN techniques for modelling of AFPM machines. The modelled LPTN is based on the work of Wrobel and Mellor in creating 3-dimensional analytical thermal models of electrical machines [8]. A notable weakness of LPTN modelling is the reliance on geometry specific correlations, especially with respect to convective terms, however for the modelling investigated, the correlations of heat transfer are well understood, having been verified in the literature experimentally and through CFD by Boutarfa [9], and Howey [10] respectively.

One variation of the AFPM machine is the YASA topology [11]. This topology is unique in that each coil core is segmented from the rest of the stator, reducing iron content, and thus increasing the power density. Due to the variations between YASA machines and other AFPM topologies, the presented models from literature are unsuitable for this analysis. YASA AFPM Machines are ideally suited to automotive traction applications due to their high torque density. Investigations into YASA machines for automotive applications have led to some recent developments, including a passively air cooled machine utilising stator housing fins completed by Winterborne et al. [11]. This method achieved a predicted peak power of 0.7kW. Additionally a liquid cooled YASA motor with IMD was developed by Mohamed et al. [7], with a predicted power rating of 17kW, utilising a distributed inverter, and water cooling channels integrated into the casing between the machine windings and the inverter module.

One method for transfer of heat between the source and the cooling system is heat pipes. They are used where the cooling requirement is high, whilst the loss producing device has a low cooling potential. Use of heat pipes additionally allows for the geometry of the cooling structure to be modified depending on the application, ensuring critical dimensions are not compromised. In this instance it is suggested that the heat pipes be used to redirect the thermal path around the rotor to enable expansion of the heat sink without further increasing the machine diameter. Heat pipes can be complicated to model, however they can be represented as a single lumped thermal resistance, typically in the region of 0.01-0.2K/W [12]. Here, typical values based on off the shelf heat pipes will be used for the thermal resistance.

II. Methodology

The investigation into LPTN's begins with identifying the machine and inverter topologies being analysed. These must be investigated in order to determine the losses, which are used as inputs to the thermal modelling. A visual representation of the process flow is given in Figure 1.

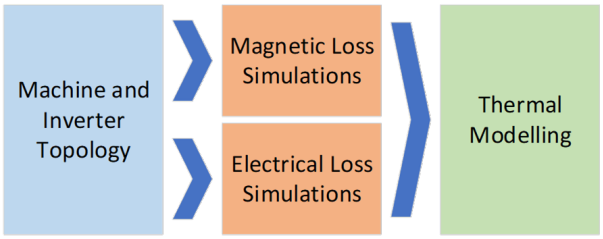

Fig. 1: Process flow for system modelling

III. Case Study Machine

A commercially available machine was selected for this project, a representation of this is given in Figure 2. This machine was originally a water cooled machine, and was selected as it is a good representation of the topology being investigated, and has good power density when compared to similar machines from literature. The machine parameters are detailed in Table I.

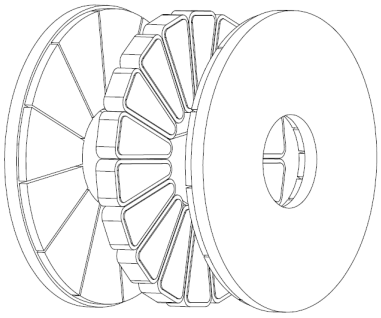

Fig. 2: Representation of the machine being examined

TABLE I: Parameters for machine examined [13]

Peak Power	Peak Torque	Max. Speed
160kW	370Nm	8000rpm

Modelling of this machine with a stator mounted heat sink and forced air cooling gave a power rating of 11kW. As multiple operating power levels are to be investigated, machine efficiency will be used as the baseline for estimating losses at each operating point.

IV. Loss Modelling

In order to develop the losses required for this analysis, electrical and electromagnetic modelling was completed in PLECS [14] and ANSYS Maxwell [15]. Representations of the loss density in the machine, and the inverter topology are shown in Figure 3 and Figure 4 respectively. The inverter

topology utilises Silicon Carbide (SiC) MOSFETs, with a peak temperature rating of 175^{o}C. For the purposes of introducing a safety factor to allow for increased life expectancy of the devices, the analysis is conducted to assume that the peak design temperature for the junction is 150^{o}C.

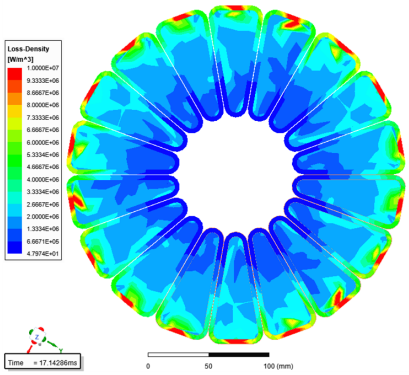

Fig. 3: Surface view of stator iron and coils with the time averaged loss density plot as an output from magnetic FEM of the motor being examined. end winding losses are consistent with observations from literature [16].

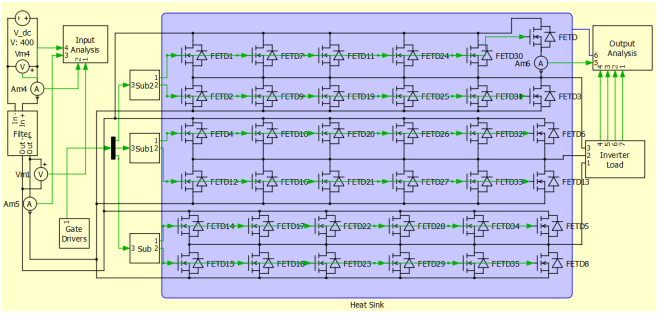

Fig. 4: PLECS model of inverter used to calculate losses, using 6 SiC MOSFETs in parallel per half bridge branch.

As the off the shelf power rating for the machine differs from the expected power rating achievable using the newly proposed air cooling method, the losses are represented in terms of the machine and inverter efficiency.

A. Magnetic Losses

For the magnetic analysis, a 1/3 angular sector of the machine was used for the analysis with virtual symmetry enabled in the software. This was done to improve computation time with minimal reduction in accuracy. From the results, as shown in Figure 5, it can be seen that the average machine losses for the 1/3 of the machine being analysed are 3.33kW for the copper and stator core combined, which becomes 9.99kW for the whole machine. This corresponds to a peak machine efficiency of 94.7%. It is also seen that the loses are concentrated on the end winding of the coil, this is an affect that has been observed in literature [16].

B. Power Electronics Losses

The PLECS electrical model was analysed using the machine's off the shelf suggested power, with a device switching

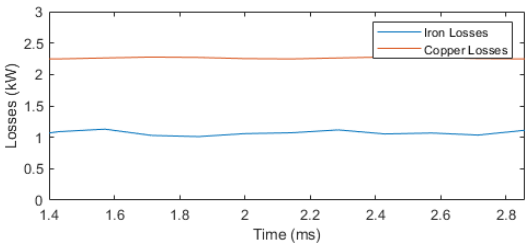

Fig. 5: Machine losses given by magnetic FEM, showing 1.07kW iron losses, and 2.26kW copper losses, for the 1/3 of the machine being analysed.

frequency of 10kHz. From the data given in Figure 6, and multiplied by the total number of devices in the machine, the total inverter losses at steady state can be seen to be 8.17kW. this corresponds to a peak inverter efficiency of 95.6%.

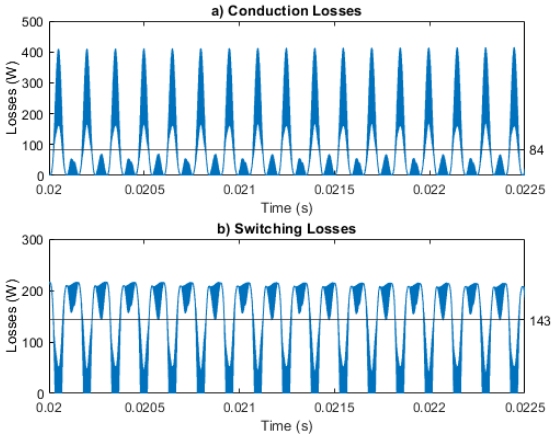

Fig. 6: Loss data from PLECS electrical modelling, showing 84W average conduction losses (a), and 143W average switching losses (b) per device for the inverter shown in Figure 4

C. Loss Summary

Table II shows the losses from the machine and drive. These will be used as inputs to the LPTN model presented in this paper.

TABLE II: IMD component losses (NOT YASA LTD. DATA)

Component	Total Power Loss	Component Efficiency
Inverter	8.17kW	95.6%
Stator Iron	3.20kW	98%
Stator Windings	6.79kW	96.4%
Total System	18.16kW	90.3%

V. Drive Integration

The IMD is modelled as a distributed inverter surrounding the stator. A similar method will be employed to that utilised by Mohamed et al. [7], where a half bridge module is placed on each individual coil, using separate PCBs for each module. A representation of this is given by Figure 7.

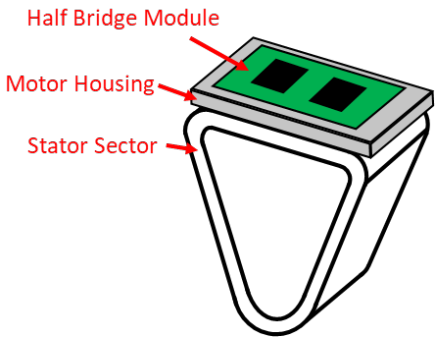

Fig. 7: Representative view of IMD concept.

As is shown in Section IV, both the motor coils and the drive produce significant losses. Placing the components in close proximity raises the additional challenge of preventing thermal runaway within either the motor or the drive. As such, it is important to ensure that the system is sufficiently cooled.

VI. Lumped Parameter Thermal Network

The LPTN approach utilises the development of a 3-Dimensional mesh of nodes connected by thermal resistances. For simplicity, it is assumed that each mesh element is cuboidal in nature [8]. For the development of this model, a single coil segment was taken as a 20^o sector of symmetry throughout the motor. This is divided into "cells" with nodes at the centre. The thermal resistance of each element is not a fixed value for each element, but rather is geometry dependent. As such, the thermal resistance must be calculated independently for each thermal path. This is given by Fourier's Law of Conduction [17]. It is assumed that radiative heat transfer is negligible for this application.

A. Application to YASA topology

In order to effectively develop this model for the YASA topology, the geometry was segmented into individual coil sections. Each coil was then sliced into layers, for which the LPTN was developed. This method was applied in Matlab [18] to build the LPTN, a representation of which is shown in Figure 8.

The model is copied into sections representing a "slice" through the model, with thermal resistances added between each section. It is further assumed that the primary cooling path is through the end windings of the machine. As such, the thermal resistance of the case must be taken into account, along with any additional components within the cooling path. This is added to the model as a separate network, modelling a single element for each relative section of the casing, and a straight thermal resistance for the path to the cold plate. Modelling of the cooling system is discussed in Section VII.

Included in this model is a segment of the rotor. For the purpose of simplicity, it is assumed that the magnets are a simple disk in the motor geometry. The magnet and rotor iron are divided into a similar network of nodes and resistances.

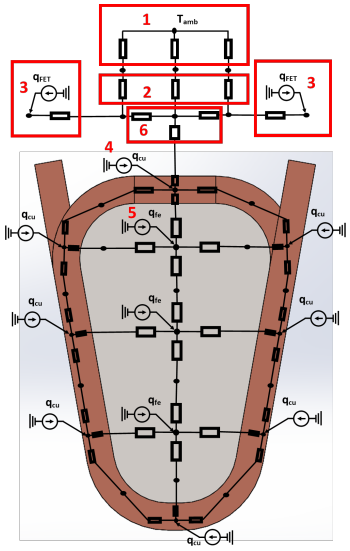

Fig. 8: Lumped Parameter Thermal Network for a single coil overlaid. Additional components are labelled: 1) Heat sink convective model; 2) Heat pipe thermal resistances; 3) MOSFET thermal models; 4) Copper loss input; 5) Iron loss input; 6) Housing.

B. Air-Gap Heat Transfer

In order to properly include the rotor within the model, the air-gap must be modelled. Air-gap heat transfer coefficients required for the LPTN have been well developed by Howey and Boutarfa in CFD and experimentally [9], [10]. From Howey, the Reynolds number for the air gap is given by:

$$Re_\theta = \frac{\omega R^2}{\nu} \tag{1}$$

In order to calculate the heat transfer for a convective system, the Nusselt number must be known. This is a highly geometry and condition specific value, and is most accurately measured experimentally, as done by Boutarfa [9].

$$Nu = 0.044 Re_\theta^{0.75} \tag{2}$$

Due to the nature of the conditions in the air gap compared to those investigated by Boutarfa, Equation 2 is used to calculate the Nusselt Number for the air gap.

VII. System Cooling

Ensuring that the drive IMD is properly cooled is essential for maintaining lifetime and efficiency of the machine. In this particular case, air cooling is being investigated as the method of machine cooling. Flat plate cooling, representing the bare outer surface of the case, as well as heat sink cooling will be investigated. The correlations for these methods are well understood, with significant experimental validation being completed historically. These are detailed by Bejan [19]. For this analysis, two air cooling methods are investigated. Firstly, flow over a flat plate, for which it is shown by Bejan that

the formula for the Nusselt Number reduces to Equation 3, where Pr is the Pradtl number for the flow.

$$Nu_x = 0.332 Re_x^{1/2} \cdot Pr^{1/3} \tag{3}$$

Secondly, the flow of air through a heat sink is investigated. For simplification of analysis, only rectangular fin heat sinks were investigated. As the spacing between fins is typically much smaller than the height of the fins, it is approximated that the flow is similar to that between parallel plates of infinite length. In this instance, the Nusselt number is defined as:

$$Nu_x = \frac{q''(x) D_h}{k[T_0 - T_m(x)]} \tag{4}$$

Where $q''(x)$ is the total heat transfer rate, D_h is the hydraulic diameter of the system, T_0 is the ambient temperature, and $T_m(x)$ is the surface temperature of the heat sink. These convection calculations are combined with the conduction through the fins to create a single lumped thermal resistance parameter to represent the heat sink behaviour. This is integrated into the machine model.

Directly mounting the heat sink to the housing limits the available surface area. Utilising heat pipes enables a remote heat sink with a greater base plate surface area, which allows for improved thermal resistance characteristics. For machine modelling, heat pipes can be simplified to a single lumped thermal resistance [12]. Conceptual visualisations for the two cooling methods being investigated are shown in Figure 9.

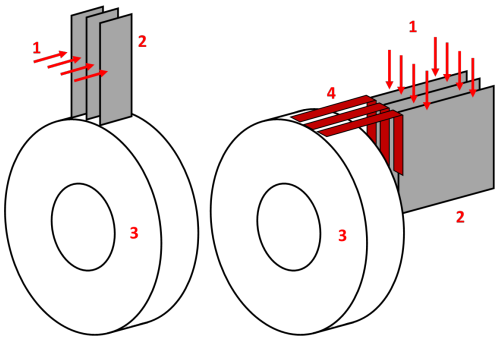

Fig. 9: Representative arrangements for the heat sink concepts investigated in this paper (Not to scale). A single representative portion of the heat sink is shown, with the final model investigating this as being patterned around the machine housing. Components are: 1) Air Flow; 2) Heat Sink; 3) Motor Housing; 4) Heat Pipes. Left: finned heat sink attached to stator housing; Right: Remote heat sink connected to housing using heat pipes.

VIII. Lumped Parameter Thermal Network Results and Discussion

The LPTN was used to simulate the thermal behaviour of the of the machine in isolation with a finned stator housing, an IMD with a finned housing, and an IMD with remote fins connected by heat pipes. Removal of the heat sink to the rear of the rotor allows for a change in the aspect ratio of the heat sink, as well as for an increase in heat sink volume that may be less impactful on the overall motor geometry. The combination of the aspect ratio change, and the volume increase would allow for a reduction in the thermal resistance of the heat sink, thus improving the thermal capabilities of the machine.

The cooling systems are analysed for air flow rates up to 40m/s, with air inlet temperature of 27°C, as these are comparable flows to velocities seen in automotive applications. Velocities beyond 40m/s are not investigated due to the diminishing returns apparent at higher air flow rates.Temperature limits for SiC devices and motor insulation are important for determining peak power. These are shown in the presented results, and used to calculate peak power given in Section VIII-D.

A. YASA Machine with Stator Mounted Heat Sink

Housing fins on the machine outer diameter are used to develop a baseline for the machine performance at varying air flow velocities. Figure 10 shows the machine can achieve up to 10kW in isolation from the power electronics at 12m/s air flow rate.

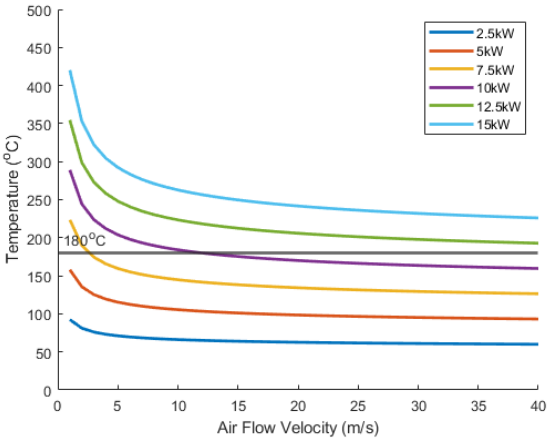

Fig. 10: Thermal behaviour of the machine various power ratings when cooled using stator housing fins. Includes the machine temperature limit of 180°C.

B. IMD with Stator Mounted Heat Sink

From the results shown in Figure 11, the IMD with housing fins can operate at a maximum power rating of 5kW with 12m/s air flow rate. This increases to 7.5kW when the air flow velocity is increased to 25m/s.

C. Optimised Remote Heat Sink

For the analysis, a heat sink was optimised for the footprint allowable in the remote application. This was found to have a fin height of 8cm. Figure 12 shows the results with this heat sink. As is shown, the IMD is predicted to be capable of achieving up to 7.5kW with air flow rates of 10 m/s, and up to 12kW for air flow rates of 36m/s.

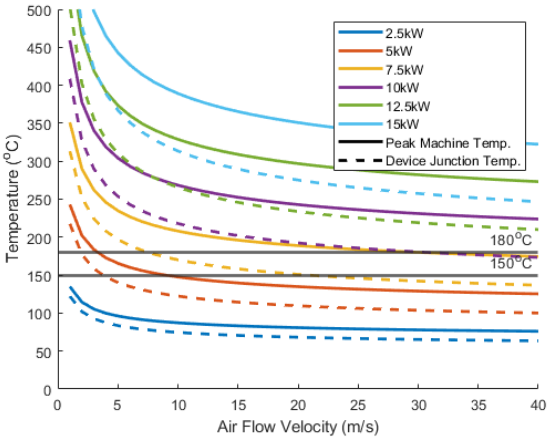

Fig. 11: Thermal behaviour of the machine and power MOSFETs in the IMD at various power ratings when cooled using a stator mounted heat sink. Includes the machine temperature limit of 180^{o}C and MOSFET Temperature limit of 150^{o}C.

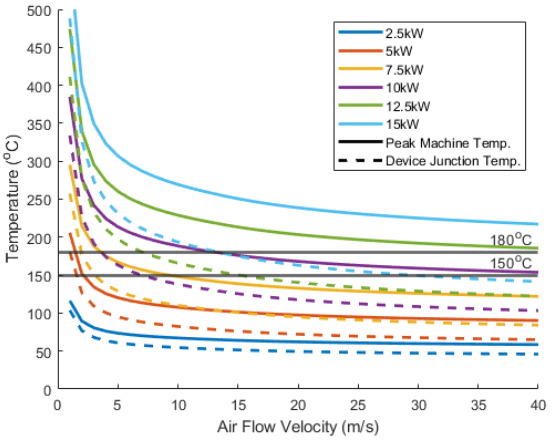

Fig. 12: Thermal behaviour of the machine and power MOSFETs in the IMD at various power ratings when cooled using a remote heat sink. Includes the machine temperature limit of 180^{o}C and MOSFET Temperature limit of 150^{o}C.

D. Cooling System Sizing

As shown, the achievable power rating of the system decreases by 27% through the integration of the drive with the machine whilst maintaining the same cooling method. Analysis of the results for machine temperatures at different power ratings suggests that using the proposed configuration, the peak performance of the machine does not increase above 10kW. This is predicted to be limited by the contact surface area of the heat sink and heat pipes with the stator coils. It is useful to provide a comparison of the machine power ratings at varied air flow velocities. This is given in Figure 13. Here, the isolated machine performance is compared with and without a stator heat sink. A 10kW power rating is achievable without a heat sink at 36m/s air flow rate, where 10kW is achievable at 12m/s when the heat sink is applied, and a peak power rating of 11kW is achievable at 36m/s. Furthermore, the IMD configuration is investigated both using the same heat sink as the isolated motor, and a range of heat sinks based on the modified aspect ratio achievable using heat pipes, with volumes between that of the ”equal volume” heat sink, and the optimised heat sink. It is shown that the peak power rating achievable using the stator heat sink is 8kW at 36m/s. Using a heat sink of equal volume, but modified aspect ratio allows the power rating to increase to 10kW at 36m/s, whilst increasing the volume of the heat sink again achieves 10kW, but at the lower flow rate of 2.5m/s, and a peak power rating of 12kW at 36m/s.

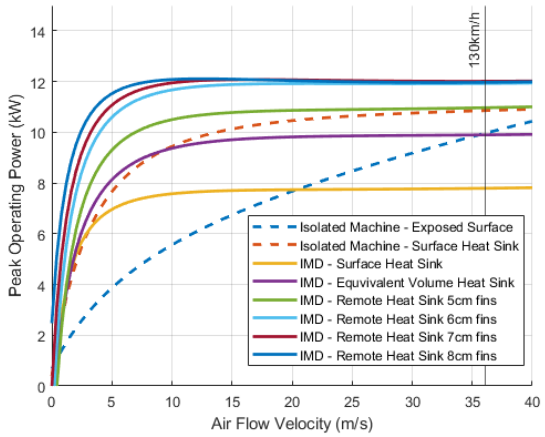

Fig. 13: Peak power for each machine configuration as a function of air flow velocity over the heat sink, with air flow velocity at 36m/s or 130km/h shown.

The primary aim of this model is to demonstrate that air cooling is a viable method for cooling a YASA IMD. It is shown that by utilising a remote heat sink at a location where the heat sink can be enlarged, the power rating compared to the machine in isolation can be matched, and exceeded. The results provide evidence that this model might be used as a starting point in the design of an air cooled YASA IMD with high power density.

IX. Conclusions

In this paper, a LPTN is discussed and developed for a YASA AFPM motor and IMD, including modelling of the air-gap heat transfer correlations. Loss data from magnetic and electrical FEM simulations are provided as inputs to the model. The model is run using thermal resistances for heat sinks modelled at varied air flow velocities, comparing the machine in isolation to the IMD. Introduction of the IMD is found to reduce the peak power of the machine by 27%, and to achieve the same power rating as the isolated machine, the IMD must utilise a remote heat sink with a modified aspect ratio. It is estimated that the heat sink can be enlarged to 2x the original volume by utilising heat pipes to redirect heat to an alternative location. Using this configuration, it is found that a steady state power rating equal to that of the machine in isolation is achievable at similar air flow velocities.

X. Acknowledgment

This work was supported by the Engineering and Physical Sciences Research Council (grant number EP/S024069/1) and by YASA Limited. The work was conducted within the Centre for Doctoral Training in Sustainable Electric Propulsion.

References

[1] T. J. Woolmer and M. D. McCulloch, "Axial Flux Permanent Magnet Machines: a New Topology for High Performance Applications," in *IET - The Institution of Engineering and Technolgy Hybrid Vehicle Conference 2006*, 2006.

[2] T. Woolmer and M. McCulloch, "Analysis of the Yokeless And Segmented Armature Machine," in *IEEE International Electric Machines and Drives Conference*, 2007.

[3] L. De Lillo, B. Ahmadi, L. Empringham, M. Johnson, J. Espina, and R. Abebe, "Next Generation Integrated Drive, NGID: A Novel Approach to Thermal and Electrical Integration of High Power Density Drives in Automotive Applications," *2018 IEEE Energy Conversion Congress and Exposition, ECCE 2018*, pp. 1228–1232, 2018.

[4] N. Rostami, M. R. Feyzi, J. Pyrhonen, A. Parviainen, and M. Niemela, "Lumped-parameter thermal model for axial flux permanent magnet machines," *IEEE Transactions on Magnetics*, vol. 49, no. 3, pp. 1178–1184, 2013.

[5] C. Corey and W. Wink, "3D Thermal Network Modeling for Axial-Flux Permanent Magnet Machines with Experimental Validation," pp. 4059–4066, nov 2021.

[6] J. F. Gieras, R.-J. Wang, and M. J. Kamper, *Axial Flux Permanent Magnet Brushless Machines*, 2nd ed. Springer Netherlands, 2008.

[7] A. H. Mohamed, H. Vansompel, and P. Sergeant, "An Integrated Modular Motor Drive with Shared Cooling for Axial Flux Motor Drives," *IEEE Transactions on Industrial Electronics*, vol. 68, no. 11, pp. 10 467–10 476, nov 2021.

[8] R. Wrobel and P. H. Mellor, "A General Cuboidal Element for Three-Dimensional Thermal Modelling," *IEEE TRANSACTIONS ON MAGNETICS*, vol. 46, no. 8, 2010. [Online]. Available: http://ieeexplore.ieee.org.

[9] R. Boutarfa and S. Harmand, "Local convective heat transfer for laminar and turbulent flow in a rotor-stator system," *Experiments in Fluids*, 2005.

[10] D. A. Howey, P. R. N. Childs, and A. S. Holmes, "Air-Gap Convection in Rotating Electrical Machines," *IEEE Transactions on Industrial Electronics*, vol. 59, no. 3, 2012. [Online]. Available: http://ieeexplore.ieee.org.

[11] D. Winterborne, N. Stannard, L. Sjoberg, and G. Atkinson, "An Air-Cooled YASA Motor for in-Wheel Electric Vehicle Applications," *IEEE Transactions on Industry Applications*, vol. 56, no. 6, pp. 6448–6455, nov 2020.

[12] S. Zimmermann, R. Dreiling, T. Nguyen-Xuan, and M. Pfitzner, "An advanced conduction based heat pipe model accounting for vapor pressure drop," *International Journal of Heat and Mass Transfer*, vol. 175, aug 2021.

[13] "YASA P400 R Series." [Online]. Available: https://www.yasa.com/products/yasa-p400/

[14] "Plecs User Manual Version 4.6." [Online]. Available: https://www.plexim.com/files/plecsmanual.pdf

[15] "Ansys Maxwell 2022 R1 User Manual." [Online]. Available: https://ansyshelp.ansys.com/account/secured?returnurl=/Views/Secured/Electronics/v221/en/Subsystems/Maxwell/Maxwell.htm{%}23Maxwell{_}PDFs.htm

[16] A. Mlot, M. Lukaniszyn, and M. Korkosz, "Analysis of end-winding proximity losses in a high-speed PM machine," *Archives of Electrical Engineering*, vol. 65, no. 2, pp. 249–261, 2016.

[17] A. Bejan and A. D. Kraus, *Heat Transfer Handbook*. John Wiley and Sons, 2003.

[18] "Matlab User Manual." [Online]. Available: https://uk.mathworks.com/help/matlab/index.html?s{_}tid=CRUX{_}lftnav

[19] A. Bejan, *Heat Transfer*, 1st ed. John Wiley and Sons, 1993.

Biographies

Alexander Jeffrey received a MEng in Mechanical Engineering from the University of Exeter in 2018. From 2018-2019, he worked as a graduate engineer in additive manufacturing, and in 2019 he began his PhD as part of the Sustainable Electrical Propulsion Centre for Doctoral Training, based in the Power Electronics Machines and Control research group at the University of Nottingham. His research focusses on thermal management of integrated motor drives.

Peter Connor received an M.Eng. and Ph.D. from the Department of Mechanical, Materials and Manufacturing Engineering Department, University of Nottingham, UK, in 2009 and 2014, respectively. He is a Senior Research Fellow in the Power Electronics, Machines and Control Research Group in the Faculty of Engineering at the University of Nottingham. His research interests are mechanical design and thermal management of electrical machines for industrial power generation and high-speed, high power-density traction and aerospace applications.

Gaurang Vakil received the Ph.D. degree in variable speed generator design for renewable energy applications from the Power Electronics, Machines and Drives Group, IIT Delhi, New Delhi, India, in 2016. He subsequently worked as a Research Associate and then Research Fellow with the Power Electronics, Machines and Controls Group, University of Nottingham, Nottingham, U.K. He was later appointed as an Assistant Professor in 2016 and then Associate Professor in 2022 at the same institution. His main research interests include design and development of high-performance electrical machines for transport and propulsion, optimizing electric drive-train for pure electric and hybrid vehicles (aerospace and automotive), high-power density machines, and magnetic material characterization. Within the research group and the university, he champions the activities around the magnetic materials and fast/precise loss modelling of electromagnetic components.

Paul Evans received the MEng degree in Electrical and Electronic Engineering, and the PhD degree in Electrical engineering from the University of Nottingham, UK, in 2007, and 2011 respectively. In 2010 he became a Research Fellow, was appointed Assistant Professor in 2013 and then Associate Professor in 2019 at the same institution. His expertise lies in the application of accelerated computational modelling techniques to the simulation of power electronic systems and his work on extraction of compact thermal models was awarded the IEEE Transactions on Power Electronics second prize paper in 2013. He currently leads the Virtual Prototyping work in the EPSRC Centre for Power Electronics.

Prof Pat Wheeler received his BEng [Hons] degree in 1990 from the University of Bristol, UK. He received his PhD degree in Electrical Engineering for his work on Matrix Converters from the University of Bristol, UK in 1994. In 1993 he moved to the University of Nottingham and worked as a research assistant in the Department of Electrical and Electronic Engineering. In 1996 he became a Lecturer in the Power Electronics, Machines and Control Group at the University of Nottingham, UK. Since January 2008 he has been a Full Professor in the same research group. He was Head of the Department of Electrical and Electronic Engineering at the University of Nottingham from 2015 to 2018. He is currently the Head of the Power Electronics, Machines and Control Research Group, Global Director of the University of Nottingham's Institute of Aerosapce Technology and was the Li Dak Sum Chair Professor in Electrical and Aerospace Engineering. He is a member of the IEEE PELs AdCom and is currently IEEE PELS Vice-President for Technical Operations. He has published over 750 academic publications in leading international conferences and journals.

Simon Hart is the CTIO (Controllers and Power Electronics) at YASA, a manufacturer of high-power density motor controllers and axial flux motors for automotive and other sectors. Simon founded the controller and power electronics group at YASA. In 2022 YASA became part of Mercedes-Benz. Before joining YASA Simon was with Emerson Control Techniques for 15 years and before that Eurotherm Drives. Simon has papers and patents in the fields of power electronics, motor control, software systems and thermal management techniques. He is an Honorary Associate Professor in Power Conversion for Transportation Electrification at the University of Nottingham.